university of groningen

University Medical Center Groningen

University of Groningen

Dynamics of Frenkel excitons in disordered molecular aggregates

Fidder, Henk; Terpstra, Jacob; Wiersma, Douwe A.

Published in:
Journal of Chemical Physics

DOI:
10.1063/1.460220

IMPORTANT NOTE: You are advised to consult the publisher's version (publisher's PDF) if you wish to cite from it. Please check the document version below.

Document Version
Publisher's PDF, also known as Version of record

Publication date:
1991

Link to publication in University of Groningen/UMCG research database

Citation for published version (APA):
Fidder, H., Terpstra, J., & Wiersma, D. A. (1991). Dynamics of Frenkel excitons in disordered molecular aggregates. *Journal of Chemical Physics*, *94*(10), 6895-6907. https://doi.org/10.1063/1.460220

Copyright
Other than for strictly personal use, it is not permitted to download or to forward/distribute the text or part of it without the consent of the author(s) and/or copyright holder(s), unless the work is under an open content license (like Creative Commons).

The publication may also be distributed here under the terms of Article 25fa of the Dutch Copyright Act, indicated by the "Taverne" license. More information can be found on the University of Groningen website: https://www.rug.nl/library/open-access/self-archiving-pure/taverne-amendment.

Take-down policy
If you believe that this document breaches copyright please contact us providing details, and we will remove access to the work immediately and investigate your claim.

Downloaded from the University of Groningen/UMCG research database (Pure): http://www.rug.nl/research/portal. For technical reasons the number of authors shown on this cover page is limited to 10 maximum.

Download date: 04-05-2023

Dynamics of Frenkel excitons in disordered molecular aggregates

Henk Fidder, Jacob Terpstra, and Douwe A. Wiersma
University of Groningen, Department of Chemistry, Ultrafast Laser and Spectroscopy Laboratory, Nijenborgh 16, 9747 AG, Groningen, The Netherlands

(Received 27 November 1990; accepted 8 February 1991)

This article reports on the optical dynamics in aggregates of pseudoisocyanine-bromide and iodide. For PIC-Br in an ethylene glycol/water glass, the results of resonance light scattering (RLS), time-resolved emission, and photon echo decay measurements are discussed. Band structure calculations based on a linear-chain model for the J aggregate have also been performed. The results show that the J band can be described as a disordered Frenkel exciton band in which *superradiant* states exist that extend over about 100 molecules. Numerical simulation studies of the J band, based on Anderson's Hamiltonian with uncorrelated diagonal site energies, show that the ratio κ of the disorder parameter D over the nearest-neighbor coupling parameter J_{12} is about 0.11. Using the frequency dependence of the ratio between the yields of vibrational fluorescence and Raman scattering as a probe, the dephasing process and derived parameters for the bath correlation function at three different temperatures have also been examined. It is shown that at all temperatures the exciton dephasing process occurs in the *fast modulation limit*. For PIC-I in a Langmuir–Blodgett film the optical excitation can be described also in terms of a band transition but the disorder is much larger than in a glass. For this system, a low-temperature fluorescence lifetime of about 10 ps is measured, which suggests that the excitation is much more delocalized than in the case of self-assembled aggregates in a glass. Resonance Rayleigh scattering experiments on PIC in a bilayer show that the exciton-dephasing rate increases dramatically at energies above the renormalized band edge.

I. INTRODUCTION

The study of the nonlinear optical properties of aggregates and polymers has recently received new momentum because of possible applications of these materials in the field of optical communication and computing.[1,2] The possibility of making ultra-thin polymeric films by epitaxial growth techniques[3] and of using the Langmuir–Blodgett technique to fabricate mono- and multilayers of aggregates[4] has further stimulated interest in this area of condensed phase spectroscopy.

We have recently started[5–8] with an optical and nonlinear optical study of aggregates in glasses and Langmuir–Blodgett (LB) films with the aim of understanding the optical dynamics and nonlinear optics of these materials in greater detail. Related work is done on polysilanes,[9–13] a class of polymers that shows great promise for many technological applications.

Aggregate research started in the midthirties with the discovery by Jelly[14] and Scheibe[15] that concentrated solutions of the dye molecule pseudoisocyanine (1,1′-diethyl-2,2′-cyanine) exhibit a very sharp transition to the red of the monomer transition. Both men ascribed this red-shifted transition, currently known as J band, to an optical excitation on aggregates of this dye molecule. Scheibe[16] made also the interesting discovery that in streaming solutions of these aggregates the J-absorption band is polarized along the stream direction. This finding clearly shows that the aggregates in solution form threadlike structures.

Following the original work of Scheibe and Jelly, numerous workers have contributed to our understanding of the structure,[17,18] optical spectrum[19–22] and dynamics[5–8,23–28] of PIC aggregates. Especially through the pioneering work of Möbius and Kuhn[4,29] in the past decade it was established that by use of the Langmuir–Blodgett technique fundamental studies on the dynamics could be done under controlled conditions. Using the fluorescence quantum yield as a probe they concluded, for instance, that the aggregate's radiative lifetime is temperature dependent and that the *radiative* lifetime is directly related to the number of molecules coherently coupled. Direct lifetime measurements on aggregates were also performed,[30,31] but in many of the early experiments too high excitation intensities were used, leading to the observation of fluorescence decay curves dominated by exciton annihilation effects. Notable exceptions are the experiments performed by Sundström *et al.*[26] on J aggregates in solution and by us[7] on aggregates in the condensed phase. These latter experiments also clearly confirmed Kuhn's and Möbius' suggestion[29] of a temperature dependent radiative lifetime of the aggregate.

Theoretically the optical absorption spectrum of the J aggregate has successfully been described in terms of an excitonic transition on a linear chain with two molecules per unit cell.[20,21] The narrow bandwidth of the origin transition of the aggregate was shown to result from motional narrowing.[19] Spano, Kuklinsky, and Mukamel[25] recently showed that this model can account not only for the optical spectrum[20,21] but also for the superradiant dynamics of PIC.

Downloaded 06 Feb 2006 to 129.125.25.39. Redistribution subject to AIP license or copyright, see http://jcp.aip.org/jcp/copyright.jsp

However, for a proper description of the temperature dependence of the radiative lifetime of PIC linear exciton–phonon coupling needs to be taken into account explicitly. Furthermore, Spano *et al.* found that use of a non-Markovian master equation is essential. An important prediction of this theory is that for strong electron–phonon coupling, the *effective* number of coupled molecules at $T=0$ saturates for large aggregates. However, the theory does not account for inhomogeneity of the J band, which is known to destroy superradiance, even in the absence of phonons.[23] Spano *et al.*'s theory predicts also that phonon-induced scattering produces a nonthermal distribution over band states by k-selective scattering. Measurement of the exciton dynamics therefore is an essential test of this theory. Also, many other questions remain regarding the optical dynamics of the J aggregate. For instance, how to explain the difference in low-temperature decay time of the photon echo and the fluorescence.[7] Furthermore, what is the mechanism of hole burning[5,27-28] and what is the nature of the quasilocalized states that exist in the J band. Finally, how does inhomogeneity affect the superradiant behavior and exciton dynamics in the system.

In order to answer these questions we have performed fluorescence lifetime, resonance light scattering (RLS) and photon echo experiments on J aggregates in glasses and LB films. The RLS spectrum of the J band of PIC in a glass shows clear evidence for a disordered band structure and allows determination of the dephasing dynamics in terms of a stochastic model. One of the main conclusions of the frequency dependence of the RLS spectrum of the J band is that exciton dephasing proceeds at all temperatures in the so-called *fast modulation* limit. From these experiments, we conclude also that the discrepancy between the low-temperature fluorescence lifetime and the photon echo decay is not due to remnant pure dephasing processes but to variations in the dipole strengths of the states in the band and relaxation processes. Computer simulations of the low-temperature line shape of the J bands have been performed, from which information on the disorder and the average number of coherently coupled molecules is obtained. These calculations provide also a clear picture of the mechanism of hole burning in the J band. Fluorescence lifetime measurements on PIC in a glass and Langmuir–Blodgett film suggest that in a two-dimensional structure the delocalization volume is much larger than in the self-assembled aggregates. The disorder in LB films, however, is also much larger which leads to much broader absorption lines than in a glass. The narrowed emission spectrum in the LB film is assigned to relaxation in the disordered band. Resonance Rayleigh scattering experiments show that the exciton-dephasing rate increases dramatically above the renormalized band edge, supporting the idea that below this edge the excitons are more localized.

II. THEORETICAL CONSIDERATIONS

A. Linear-chain exciton Hamiltonian for disordered systems

The effective Hamiltonian that describes the optical excitation on a molecular aggregate in the presence of disorder has the following well-known form:[32-33]

$$\mathbf{H}=\mathbf{H}_{ex}+\mathbf{H}_{ph}+\mathbf{H}^{(1)}_{ex-ph}+\mathbf{H}^{(2)}_{ex-ph}, \tag{1}$$

where

$$\mathbf{H}_{ex}=\sum_n(\langle\epsilon\rangle+D_n)a_n^+a_n+\sum_{m,n}J_{mn}a_m^+a_n, \tag{2}$$

$$\mathbf{H}_{ph}=\sum_q\hbar\omega_q(b_q^+b_q+1/2), \tag{3}$$

$$\mathbf{H}^{(1)}_{ex-ph}=\sum_{q,n,m}{}'F^q_{nm}\hbar\omega_q(b_q^++b_{-q})a_n^+a_m, \tag{4}$$

$$\mathbf{H}^{(2)}_{ex-ph}=\sum_{q,n}\chi^q_n\hbar\omega_q(b_q^++b_{-q})a_n^+a_n. \tag{5}$$

In Eqs. (2)–(5) the Pauli operator a^+ (a) creates (annihilates) an electronic excitation of energy ($\langle\epsilon\rangle+D_n$) at site n. D_n represents the inhomogeneous shift from the average molecular excitation energy $\langle\epsilon\rangle$; it is assumed to be randomly distributed according to a Gaussian $P(D_n)\propto\exp[-D_n^2/2D^2]$. J_{mn} stands for the dipolar coupling between molecules m and n and is scaled to the nearest-neighbor coupling term J_{12}, which for PIC has been determined to be about $-600\ \mathrm{cm}^{-1}$. The transition dipole of each eigenstate is calculated from the eigenvectors, whereby the site transition dipole is assumed to be aligned along the chain axis. The Bose operator b_q^+ (b_q) creates (annihilates) a phonon of wave vector q and frequency ω_q. $\mathbf{H}^{(1)}_{ex-ph}$ stands for the electron–phonon coupling term that expresses the lattice-vibrational dependence of J_{mn}, while $\mathbf{H}^{(2)}_{ex-ph}$ represents the dependence of the electronic excitation energy to local lattice distortion.

One of the important questions we wish to answer is to what extent the optical excitation is *delocalized* over the molecules of the aggregate chain. By a delocalized state, we mean a state whose wave function extends over several molecules. The driving term for delocalization of a single-molecule excitation to other molecules on the chain is J_{mn}, the intermolecular dipolar coupling term. A counterforce against delocalization presents the local inhomogeneity D which, especially in the case of amorphous solids, may be quite appreciable. However, in the case that the inequality $J_{12}\gg D$ holds, where D is the standard deviation of the inhomogeneous Gaussian distribution of site energies D_n, the optical excitation, in the absence of phonons, can still encompass many molecules on the aggregate. When the lattice vibrations are considered the situation becomes more complex. In the case where $J_{12}\gg D$ and the coupling of the electronic excitation with the phonons is weak, the inequality $\mathbf{H}^{(1)}_{ex-ph}\gg\mathbf{H}^{(2)}_{ex-ph}$ is obeyed. In this situation delocalized excitations are created which undergo elastic and inelastic scattering through collisions with phonons. It has previously been shown that this is exactly the situation that pertains to the J aggregate.[5-8]

The description of the line shape function of disordered Frenkel excitons has been dealt with by several groups. Knapp[19] showed, using probability calculus, that in the case of uncorrelated diagonal Gaussian disorder the inhomogeneous line profile of the dipole-allowed excitonic state should narrow by a factor of $N^{1/2}$ compared to the monomer spec-

Downloaded 06 Feb 2006 to 129.125.25.39. Redistribution subject to AIP license or copyright, see http://jcp.aip.org/jcp/copyright.jsp

trum. N is the number of coupled molecules in the aggregate. Klafter and Jortner[34] used the average t-matrix approximation to describe the line shape of the disordered linear chain exciton of 1,4-dibromonaphthalene (DBN) including phonon scattering processes. This study clearly showed that in the presence of disorder the line shape can be very asymmetric due to disorder-induced mixing between the dipole allowed k state (of the perfect crystal) and other k states. Klafter and Jortner also showed that for one-dimensional systems the absorption spectrum exhibits a Lorentzian energy dependence at the high-energy side and a Gaussian wing on the low-energy side. This finding confirms the earlier conclusion of Burland *et al.*[35] that for DBN the Lorentzian wing of the exciton line shape is not caused by homogeneous dephasing but crystal imperfections. Schreiber and Toyozawa[36] were the first to perform numerical calculations on the exciton absorption line shape under the effect of lattice vibrations. Exciton systems of all dimensions were considered but only nearest-neighbor coupling was accounted for. One of the interesting conclusions was that, irrespective of the system's dimensionality, excitons become more localized near the *renormalized* band edge and furthermore that these excitons carry giant oscillator strengths.[37] Recently, Huber,[22] using a similar theoretical approach as Klafter and Jortner, studied also the effect of inhomogeneity on the frequency shift and linewidth of the $k = 1$ Frenkel exciton state.

In this paper, we discuss results of calculations on a disordered linear chain Frenkel exciton in the absence of phonon scattering. The difference with Knapp's work[19] and that of Klafter and Jortner[34] or Huber[22] is that we perform numerical calculations of the eigenstates as Schreiber and Toyozawa[36] did. The calculations were performed on a linear chain consisting of a large number of molecules with random diagonal energies but with constant off-diagonal coupling constants. We have studied the effect of using only nearest-neighbor coupling and of using *all* dipolar couplings on the chain. In the latter case, the eigenstates are more extended on the chain and thus acquire more oscillator strength. The calculations are done for a large number of different sets of diagonal energies, distributed according to a preset Gaussian width. The details of these calculations will be published elsewhere.[38]

In conclusion of this section, we note that Tilgner *et al.*[13] have also performed numerical calculations of excitonic states in a disordered linear chain of polysilane. In this polymer, the excitonic disorder is much larger than for the case of PIC aggregates in a glass.

B. Resonance Raman scattering and dephasing-induced fluorescence

It is well known that resonance light scattering (RLS) spectroscopy can be used to obtain dynamical information on molecules[39,40] and excitonic systems.[41] For instance, for a two-level system it has been shown[39] that for the Markovian and low-field limits, the ratio of fluorescence and Rayleigh yields, R_M, equals $2T_1/T_2^*$. Here, T_1 is the population and T_2^* the pure dephasing time constant. For a three-level Markovian system the same relation is obtained[40,42] for the relative intensities of the vibrational fluorescence and Raman scattering, provided that the pure dephasing parameters at the different transitions are correlated:

$$\Gamma_{23}^* = \Gamma_{12}^* + \Gamma_{13}^*. \tag{6}$$

Here, the pure dephasing parameter Γ_{ij}^* refers to the transition $i \leftarrow j$.

When the optical Bloch equations are used for a description of the system's dynamics one finds that the ratio R_M is independent of frequency detuning, in contrast to observations. To remedy this situation, a non-Markovian master equation is needed to describe the time dependence of the density matrix. Ron and Ron,[43] DeBree,[42] and Mukamel[44] have shown how by use of such a non-Markovian master equation a frequency dependence of the RLS spectrum can be derived. For the so-called COP master equation the resulting expression for the relative yields of fluorescence and Raman is given by[42-43]

$$R_{nM}^{\mathrm{COP}} = 2T_1\Delta^2\tau_c/[1 + (2\pi\delta)^2\tau_c^2], \tag{7}$$

where Δ and τ_c are parameters that characterize the bath correlation function:[45] $A(\tau) = \Delta^2 \exp(-\tau/\tau_c)$, and δ is the off-set frequency (in frequency units).

Equation (7) shows that R_{nM}^{COP} is dependent on the detuning between the exciting laser and the peak of the absorption, in contradistinction to what is obtained from the Bloch equations where $R_M = 2T_1/T_2^*$, independent of detuning. Equation (7) shows also that in the impact limit $\delta\tau_c \ll 1$, R_{nM}^{COP} reduces to R_M.

The effect of inhomogeneous broadening on the RLS spectra was taken into account by convoluting the product of R_{nM}^{COP} and the homogeneous line shape function, derived from the photon echo experiments, with a Gaussian of 25-cm^{-1} FWHM width. To normalize this quantity the convoluted product was divided by the convolution of the Gaussian and the homogeneous (Lorentzian) line shape.

C. Resonance Rayleigh scattering

Hegarty *et al.*[41] showed that intense resonance Rayleigh scattering can be observed from inhomogeneously broadened excitonic transitions in quantum well structures of GaAs/AlGaAs. The high efficiency of Rayleigh scattering in these systems derives from spatial fluctuations in the refractive index. The inhomogeneously broadened exciton band is the envelope of homogeneous exciton wave packets, each homogeneous packet corresponding to a particular thickness of the quantum well. When the laser is resonant with one homogeneous transition it is off resonance with the others. Because of the strong dispersion near an excitonic transition this effect produces spatial fluctuations of the refractive index. It was also shown that in case the homogeneous width is much less than the inhomogeneous width, the Rayleigh scattering intensity can be expressed as

$$I_{RS}(\omega) \propto K[1 - \exp(-2\alpha(\omega)d]\mu^2(\omega)T_2(\omega). \tag{8}$$

Here, $\alpha(w)$ is the absorption coefficient, d the sample thickness, and $\mu(\omega)$ and $T_2(\omega)$ the frequency-dependent transition dipole moment and dephasing time. K is a constant which is proportional to the volume of the scattering entity.

Downloaded 06 Feb 2006 to 129.125.25.39. Redistribution subject to AIP license or copyright, see http://jcp.aip.org/jcp/copyright.jsp

In our LB films, we have observed very intense Rayleigh scattering signals when near-resonance excitation was employed. We attribute this effect also to spatial fluctuations in the index of refraction caused by the effects of "inhomogeneous" broadening of the aggregate's transition and strong resonant dispersion. Due to the appreciable size of the domains over which the excitation is delocalized the Rayleigh scattering efficiency can be remarkably high. We have used this effect to obtain qualitative information regarding the exciton dynamics in the disordered band. It is expected that Rayleigh scattering can also be used to explore exciton dynamics in polymers like polysilane and polydiacetylene.

III. EXPERIMENTAL SECTION

The dyes PIC-Br and PIC-I were obtained from Exciton and Kodak respectively, and used without further purification. Aggregates of PIC-Br were prepared as described in Ref. 5. Langmuir–Blodgett (LB) films of PIC-I were made using the adsorption method.[46] Doubly distilled water was used for the subphase (pH 8, $T = 20$ °C) in which PIC-I was dissolved at a concentration of 10^{-4} M. After drop-wise adding a 1.5×10^{-3}-M solution of arachidic acid in chloroform, a PIC layer is formed by adsorption to the arachidic acid monolayer. Hereafter, the two layers were transferred at a ratio of about one to hydrophobic glass slides at a pressure of 30 mN/m. The glass slides had been made hydrophobic by covering them with five monolayers of arachidic acid.

Resonance light scattering (RLS) experiments on PIC-Br were performed using a R6G dye laser pumped by a cw argon ion laser operating on all lines. With a Lyot filter and an etalon in the cavity a typical bandwidth of ≈ 0.5 cm^{-1} was obtained. Resonance Rayleigh scattering (RRS) experiments on PIC-I in a bilayer LB film were performed with a synchronously pumped picosecond dye laser using solutions of sodium fluorescein or rhodamine-6G as lasing media. The scattered light was collected at right angles with respect to the exciting beam and detected using a Spex 1402 double monochromator equipped with a RCA C31034A-02 single photon counting tube. Excitation powers used in the RLS experiments on PIC-Br varied from 2 mW on resonance to 60 mW off resonance focussed to a spot size of 0.03 mm^2. In the RRS experiments excitation intensities of less than 10^9 photons per pulse cm^{-2} were used.

The time resolved fluorescence measurements were performed with the single photon counting system described in Ref. 7. The cavity dump rate was 94 kHz and the excitation wavelength was 565 nm. The system response was improved from 70 to 35 ps by using a Zeiss M4 Q III prism monochromator instead of the grating monochromator employed in Ref. 7. Intensity-dependent measurements were performed on the double layer PIC samples at temperatures ranging from 1.5–298 K. These measurements show no intensity dependence with excitation densities ranging from 5×10^9 to 1.5×10^{12} photons per pulse cm^{-2}. In most measurements, an excitation density of about 10^{11} photons per pulse cm^{-2} was used.

Eigenvalue and eigenvector calculations of 100×100 and 250×250 real symmetrical matrices, with random Gaussian diagonal disorder were performed on a Vax 11/750 computer. The basic programs were taken from Ref. 47. The output of the diagonalization program conserves the oscillator strength and the trace better than 0.01%. It reproduces also correctly the theoretical spectrum for the homogeneous case.

IV. RESULTS AND DISCUSSION

Figure 1 shows the absorption spectra of the J bands of PIC-Br in an ethylene glycol/water glass at 4.2 and 150 K. Similar type bands have also been observed with chloride or iodide as counter ions,[26–28] but the relative intensities of the two bands depend strongly on the counter ion and on the speed of forming the glass. Also the width of the absorption bands varies slightly with cooling procedures. It has been well established[5] that these two bands are due to different aggregates of PIC but the precise nature of the structural difference is not known. It has been suggested that these bands are due to cis and trans isomers of PIC aggregates.[48] We note also that the integrated intensities of these bands up to 150 K is independent of temperature. This fact implies that in this temperature region the Franck–Condon factor remains constant, which is of importance to the analysis of the resonance light scattering spectra to be discussed below.

The temperature dependent homogeneous width and shift of these J bands, displayed in Fig. 2, have recently been discussed[5,8,27] in terms of linear exciton–phonon coupling involving a low-frequency phonon and two high-frequency optical phonons (molecular vibrations) acting as doorway states. Davydov and others[33,49] have shown that the frequency-dependent homogeneous width $\Gamma(\mathbf{k},\omega)$ and shift $\Delta(\mathbf{k},\omega)$ take the following form for the case of linear exciton–phonon coupling:

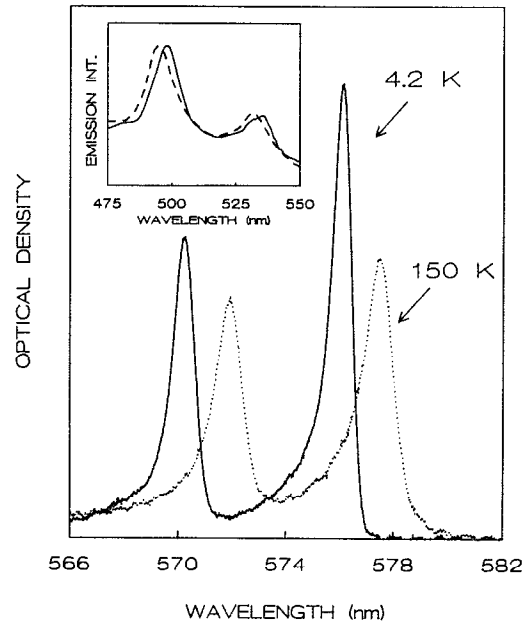

FIG. 1. Absorption spectrum of PIC-Br in an ethylene glycol/water glass at 4.2 K (—) and 150 K (···). The insert shows fluorescence excitation spectra, with fluorescence detected at the red (—) and blue (– –) site.

Downloaded 06 Feb 2006 to 129.125.25.39. Redistribution subject to AIP license or copyright, see http://jcp.aip.org/jcp/copyright.jsp

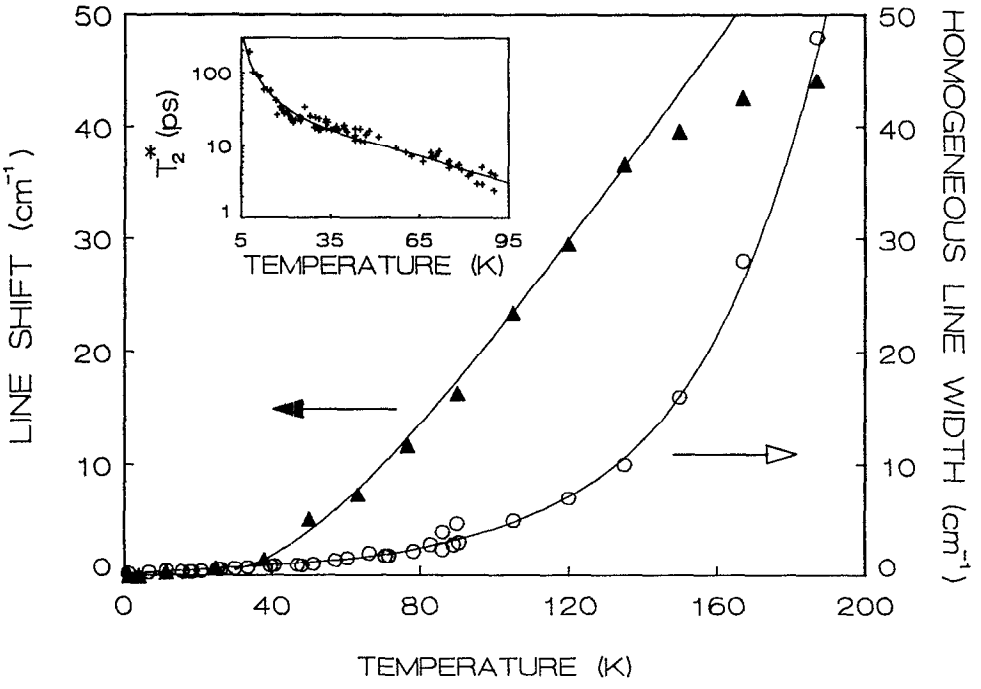

FIG. 2. Temperature dependence of the homogeneous linewidth (○) and line shift (▲) for the red excitonic origin of PIC-Br. The solid lines are fits based on Eqs. (9a) and (9b) with parameters given in the text. The insert shows the low temperature *pure* dephasing time (T_2^*) data (+); in the fit the same parameters are used as with the homogeneous linewidth.

$$\Gamma(\mathbf{k},\omega) = \frac{2\pi}{N}\sum_{qs}|F_s(\mathbf{k},\mathbf{q})|^2\{\bar{\nu}_{qs}\delta[\omega - E(\mathbf{k}+\mathbf{q}) + \Omega_s(\mathbf{q})] + (\bar{\nu}_{qs}+1)\delta[\omega - E(\mathbf{k}+\mathbf{q}) - \Omega_s(\mathbf{q})]\}, \quad (9a)$$

$$\Delta(\mathbf{k},\omega) = \frac{P}{N}\sum_{qs}|F_s(\mathbf{k},\mathbf{q})|^2\left(\frac{\bar{\nu}_{qs}}{[\omega - E(\mathbf{k}+\mathbf{q}) + \Omega_s(\mathbf{q})]} + \frac{(\bar{\nu}_{qs}+1)}{[\omega - E(\mathbf{k}+\mathbf{q}) - \Omega_s(\mathbf{q})]}\right). \quad (9b)$$

Here, $F_s(\mathbf{k},\mathbf{q})$ is the exciton–phonon interaction matrix element for an exciton with wave vector $\mathbf{k}$ and a phonon of branch s with wave vector $\mathbf{q}$. $\bar{\nu}_{qs}$ is the thermal (Bose–Einstein) occupation number for phonons, $E(\mathbf{k}+\mathbf{q})$ is the energy of the exciton after scattering, and $\Omega_s(\mathbf{q})$ is the phonon energy. N is the number of molecules that are coherently coupled and P in Eq. (9b) denotes the principal value. The terms in Eqs. (9) containing the factor $\bar{\nu}_{qs}(\bar{\nu}_{qs}+1)$ describe absorption (emission) of a phonon by the exciton with wave vector $\mathbf{k}$. For a linear chain with a negative nearest-neighbor coupling term, as is assumed to be the case for PIC, the optically allowed level is at the bottom of the band. This eliminates phonon emission contributions to the homogeneous width of the excitonic transition [the second term in Eq. (9a)]. For the line shift, as Eq. (9b) shows, all exciton–phonon scattering processes contribute, and the second term in Eq. (9b) is always of importance. The solid lines in Fig. 2 are simulations to our data based on the first terms in Eqs. (9a) and (9b). In the case of the homogeneous line width three phonons of 9 cm^{-1}, 305 cm^{-1}, and 973 cm^{-1} are needed to fit the data. We note that the value of the low-frequency mode needed in the fit is very similar to the one reported earlier.[5] The line shift up to 135 K, can be simulated using one phonon with a frequency of 100 cm^{-1}; the saturation of the shift observed above 135 K, however, cannot be explained. Our low-temperature line shift data are not accurate enough to probe the effect of a low-frequency phonon. A more extensive discussion of the line shift and line width data and the fitting parameters can be found in Ref. 8.

From room temperature circular dichroism measurements[17] and low-temperature fluorescence excitation experiments[7] is has been concluded that the J aggregate exhibits absorptions also at about 535 and 495 nm. The insert in Fig. 1 shows these bands in a glass as observed in a fluorescence excitation experiment. The band at 535 nm has been interpreted as a vibronically congested transition and the 495-nm band as a transition to the top of the exciton band.[20–21] The relative intensities of these bands compared to the origin transition, however, is not known accurately because these bands overlap with monomer and dimer absorption lines. We attribute the much larger width of these bands compared to the origin transition to radiationless relaxation. When the upper bandedge is assumed to be homogeneously broadened a 12-fs decay time for these excitons is calculated.

Figure 3 shows the low-temperature absorption and emission spectra (excited at 573 nm) of the red J band of PIC-Br. Most noteworthy is the fact that the emission spectrum tracks the absorption spectrum except for the blue edge. This phenomenon shows two things: first, that the electron–phonon coupling is weak, and second, that radiative decay successfully competes with relaxation among the states in the J band, except for excitons absorbing at the blue side of the band. As the excitation process populates all states in the band below the excitation wavelength, the observed emission line shape profile is due to the combined effects of feeding, relaxation and emission. We end by noting that the blue J band shows exactly the same behavior.

Figure 4 portrays the low-temperature photon echo and deconvoluted fluorescence decays after vibronic excitation.

Downloaded 06 Feb 2006 to 129.125.25.39. Redistribution subject to AIP license or copyright, see http://jcp.aip.org/jcp/copyright.jsp

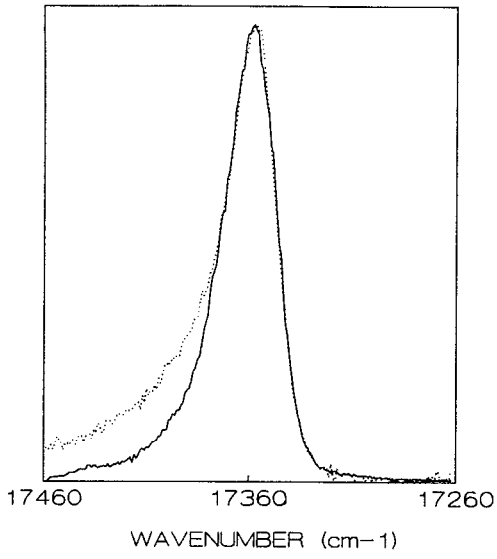

FIG. 3. Relaxed fluorescence spectrum (—), excited at 573 nm, and absorption spectrum (···) of the red site of PIC-Br at 1.5 K.

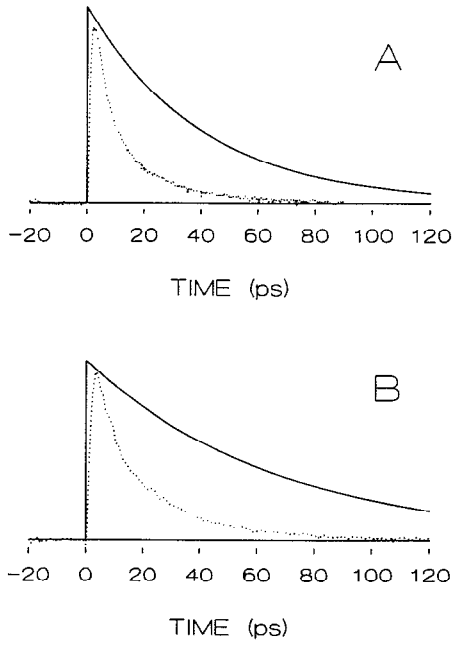

FIG. 4. Accumulated photon echo decay (···) and deconvoluted fluorescence decays (—) at 1.5 K for both the blue (a) and red (b) site of PIC-Br in ethylene glycol/water glass. The decay constants for the blue site are: fluorescence: 40 ps, echo: 6.6 ps (weight 0.75), and 25 ps; for the red site: fluorescence: 70 ps, echo: 9.4 ps (weight 0.6) and 30 ps.

From resonance Raman experiments, discussed below, it was established that the difference between the decays is not caused by *pure* dephasing processes. For a homogeneous circular aggregate, where the $k=1$ level is the only dipole-allowed state in the band, it is easy to show that, in the absence of pure dephasing processes, the photon echo and fluorescence decay should be identical. For a homogeneous linear aggregate the situation is different as more k levels carry oscillator strength. For the time-dependent fluorescence intensity after incoherent population of the band states and with no communication among these states, the following expression is obtained:[23]

$$I_{fl}(\mathbf{r},t) = Ms(\mathbf{r}) \sum_{k=1}^{N} \left(\frac{2}{N+1}\right) \cot^2\left(\frac{k\pi}{2(N+1)}\right) \times \exp[-2\Gamma_k^L t], \tag{10}$$

with

$$\Gamma_k^L = (\gamma/2)[8/(k\pi)^2](N+1) \quad k = \text{odd}, \tag{11a}$$

$$\Gamma_k^L = 0 \quad k = \text{even}. \tag{11b}$$

In Eq. (10), M is a constant and $s(\mathbf{r})$ a directional factor. γ in Eq. (11a) is the radiative rate constant of a single dye molecule.[23]

For the decay of the homodyne detected accumulated photon echo, one obtains

$$I_{\mathrm{APE}}(\mathbf{r},t) = Ms(\mathbf{r}) \sum_{k=1}^{N} \dagger \left(\frac{2}{N+1}\right)^2 \cot^4\left(\frac{k\pi}{2(N+1)}\right) \times \mathrm{Re}(\exp\{[i(\omega_k^L - \omega_1^L) - \Gamma_{2k}^L)t]\}) \tag{12}$$

with

$$\hbar\omega_k^L = \epsilon_k^L = 2J_{12}\cos[k\pi/N+1] \quad k = 1, N \tag{13}$$

Note that Eqs. (10)–(13) are based upon neglect of all couplings except the nearest-neighbor coupling term and absence of inhomogeneity.

In Eq. (12), $\Gamma_{2k}^L = \Gamma_{2k}^{*L} + \Gamma_k^L$ is the optical dephasing rate of the excitonic transition involving level k. Γ_{2k}^{*L} is the pure dephasing rate and $2\Gamma_k^L$ the population relaxation rate of this two-level system. Also, $1/2t$ is the time between the first and second excitation pulses and the dagger in the summation of Eq. (12) indicates that only odd values of k should be counted. Equation (12) shows that in the photon echo decay, in contrast to the fluorescence decay [Eq. (10)], interference effects show up due to emission of different dipole-allowed k states. Moreover, in the photon echo, states with the largest oscillator strength contribute more to the signal. Henceforth, the average decay of the photon echo will be faster than the fluorescence decay for an excitonic system with more than one dipole-allowed state in the band. We will show below that in the case of the J-aggregate local disorder spreads the oscillator strength over many states in the band. This fact is therefore partly responsible for the difference in the low-temperature decay of the photon echo and the fluorescence. Intraband relaxation is another phenomenon that should be taken into account in a description of the dynamics. It leads to shortening of the photon echo decay but to a lengthening of the radiative lifetime. We conclude that these facts together are responsible for the difference between the low-temperature photon echo and fluorescence decay.

Figure 5 shows the temperature dependence of the *measured* fluorescence lifetimes of both the red and blue aggregate absorption. In order to convert these fluorescence lifetimes to *radiative* lifetimes, the temperature-dependent quantum yields of emission are needed. Gruhl *et al.*[50] showed that for PIC in LB films the low-temperature fluorescence quantum yield is near unity. These experiments

Downloaded 06 Feb 2006 to 129.125.25.39. Redistribution subject to AIP license or copyright, see http://jcp.aip.org/jcp/copyright.jsp

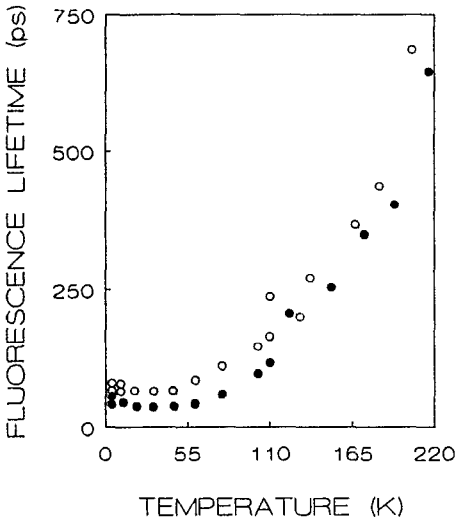

FIG. 5. Fluorescence decay time as a function of temperature for the blue (●) and red (O) excitonic origins of PIC-Br.

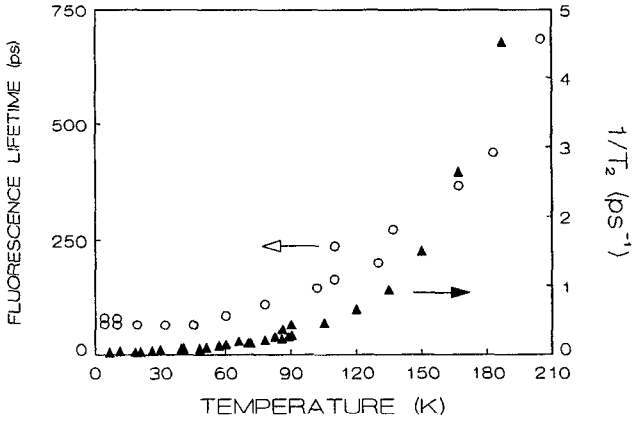

FIG. 6. Temperature dependence of the fluorescence lifetime (O) and inverse homogeneous dephasing time (▲) for the red excitonic transition of PIC-Br.

suggest that for PIC aggregates in glasses the low-temperature quantum yield should be close to 1 also, which implies that the low-temperature lifetime is the *radiative* lifetime of the aggregate. Preliminary measurements show that the fluorescence quantum yield does not change markedly with rising temperature. This fact assures that the fluorescence lifetime lengthening effect above 50 K is solely due to an increase of the *radiative* lifetime of the aggregate. Absolute fluorescence quantum yield measurements are underway to enable calculation of the absolute value of the radiative lifetime of the J aggregate. We note that the same temperature effect on the radiative lifetime has been observed in quantum well structures.[51] For both semiconductor and aggregate-excitonic systems this effect can be understood as resulting from a dilution of the oscillator strength by transfer of the population from the dipole-allowed state to other subradiant states in the band. This population-transfer effect is caused by exciton–phonon scattering which determines also the exciton's optical dephasing process. A strong correlation between the temperature dependence of the *radiative* lifetime and the *homogeneous* width of the excitonic transition is therefore expected. For the J aggregate, this correlation is shown in Fig. 6. Figure 6 shows that the radiative lifetime above 50 K is roughly proportional to the homogeneous width of the excitonic transition. Below 50 K, the radiative lifetime of the exciton is constant. Fidder *et al.*[8] have recently reported an expression for the temperature dependence of the fluorescence intensity for a homogeneous aggregate. In the case where the scattering between the different excitonic states is fast enough to maintain thermal equilibrium and the pure dephasing lifetime is much less than the low-temperature superradiant lifetime $N\gamma$, the fluorescence intensity is found to be

$$I_F(t,T) \propto \exp\left(-N\gamma \frac{f(1,T)}{\Sigma f(\mathbf{k},T)} t \right). \tag{14}$$

Here, N is the number of coupled molecules and γ the monomer's radiative rate. $f(\mathbf{k},T)$ is the Boltzmann population of the aggregate's exciton with wave vector $\mathbf{k}$, and the summation extends over all $\mathbf{k}$ in the first Brillouin zone, so that $\Sigma f(\mathbf{k},T)$ is the partition function of the exciton band. For $T \to \infty$, this equation predicts the aggregate's fluorescence lifetime to converge to the monomer's. However, calculations show that application of Eq. (14) to a linear chain does not at all account for the observed temperature dependence of the fluorescence lifetime in PIC.[8] However, the temperature independence of the fluorescence lifetime below 50 K can be understood on basis of a disordered exciton band description of the J band to be discussed below. As long as the exciton population resides within the part of the band that is optically allowed, we expect no change in fluorescence lifetime. This is borne out by the results displayed in Fig. 6. It is clear that disorder has to be taken into account to describe the superradiant dynamics of the system. We end this discussion by noting that Spano, Kuklinsky, and Mukamel[25] have recently succeeded in reproducing the temperature dependence of the fluorescence lifetime by taking account of linear exciton–phonon coupling at a microscopic level and by assuming the aggregate to be homogeneous. As will be shown below this latter assumption certainly is incorrect for PIC but the consequences for the Spano *et al.*'s theory cannot be assessed easily. For a detailed discussion of this subject we refer to the relevant paper of the Mukamel group.[25]

We now present the results of our eigenstate calculations. Figure 7 shows the comparison between the measured and simulated absorption spectrum of the J aggregate at low temperature. The simulations were performed as described in Sec. II. This particular line shape results from calculations of a linear chain composed of 250 molecules with a nearest-neighbor coupling of $-600\ \mathrm{cm}^{-1}$ and a disorder parameter D of $64\ \mathrm{cm}^{-1}$. The rather "noisy" nature of the simulated spectrum is due to the limited number of matrices (500) that were diagonalized to obtain the spectrum. Many calculations with varying numbers of molecules and other parameter sets were performed and will be discussed elsewhere.[38] In this paper, we will concentrate on the best results obtained so far. We emphasize that in this calculation not only nearest-neighbor coupling was taken into account, but that dipo-

Downloaded 06 Feb 2006 to 129.125.25.39. Redistribution subject to AIP license or copyright, see http://jcp.aip.org/jcp/copyright.jsp

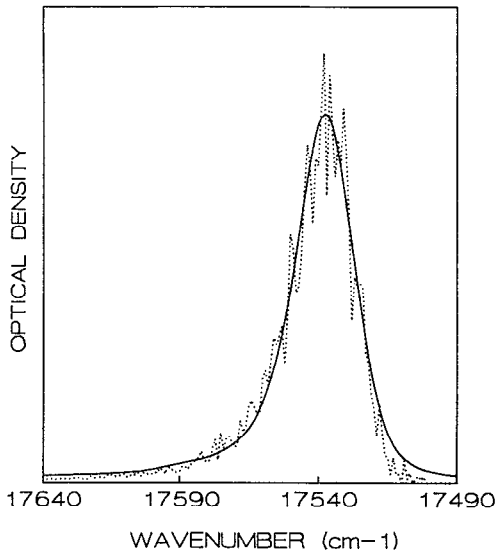

FIG. 7. Measured (—) and calculated (···) absorption spectrum of the blue site of PIC-Br. The calculated spectrum is the results of diagonalizing 500 matrices of 250 molecules, with $V = -600\ \mathrm{cm}^{-1}$ and $D = 64\ \mathrm{cm}^{-1}$. All dipolar couplings were included.

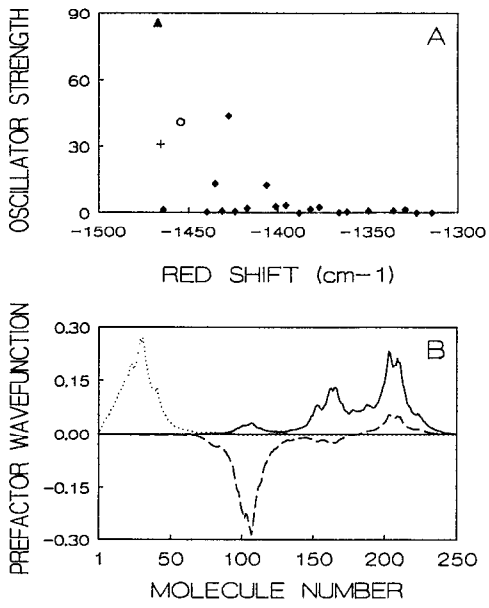

FIG. 8. (a) Eigenvalues and corresponding oscillator strengths at the lower bandedge for one chain of 250 molecules with diagonal disorder. (b) Eigenvectors corresponding to states marked in (a): (▲→—), (○→···), (+ →– –).

lar couplings involving *all* molecules on the chain were included. Inclusion of all dipolar couplings does not affect so much the line shape but has a significant effect on the delocalization of the excitation. Figure 7 shows also that disorder leads to a Lorentzian line profile on the blue edge of the J band as earlier found from perturbative[19,34] and numerical[36] calculations. Also note that the disorder of the glass has red shifted the "excitonic" transition about 10 cm^{-1} compared to the homogeneous case. Following Schreiber and Toyozawa,[36] we will refer to the peak of this excitonic transition as "renormalized band edge." Figure 8 shows the oscillator strength and site amplitudes of eigenstates near the bottom of the band chosen from one of the 500 matrices that were diagonalized. The figure shows that only a few states close to the band edge contain appreciable oscillator strength and that these states are *localized* on segments of the chain. Note that the presence of diagonal disorder is sufficient to generate localized states on a chain and that the formation of "kinks" to obtain this effect is not essential.[9] The localized nature of these excitonic states is further demonstrated by the fact that removal of 50 molecules from either end of the chain or changing the inhomogeneity in these segments hardly affects the wave functions of the states that are localized at other segments of the chain. Moreover calculations for $D/J_{12} = 0.11$ show that changing the number of molecules in the calculation from 250 to 100 only slightly affects the results. The conclusion therefore is that the *effective number* of coupled molecules saturates for chain lengths longer than about 100 molecules. It is to be noted here that Schreiber and Toyozawa[36] showed that the *subradiant* states in the band are more delocalized. This finding is especially relevant concerning the dynamics of excitons above and below the renormalized band edge.

Our calculations also suggest an explanation for the hole burning effect in the J band. Excitation of band states most likely changes the local disorder. This results in new eigenstates at other frequencies in the J band and a hole in the absorption spectrum at the excitation frequency. This shifting of oscillator strength should not affect the total oscillator strength of the J band, in agreement with a report by Hirschmann *et al.*[28] The calculations further show that the average oscillator strength per state in the low energy region is 49 times that of a monomer. The low-temperature *radiative lifetime* of a Boltzmann population in this band is thus predicted to be a factor of 49 shorter than the monomer's radiative lifetime. This prediction is in good agreement with the fluorescence lifetime obtained for the red site but about a factor of two lower than is measured for the blue site. However, in both cases the line shape of the J bands can be described with about the same D/J_{12} value. This fact demonstrates that the absorption line shape is not sensitive to details of the band structure. An extended structure of the aggregate, for instance fractal, may have little effect on the line shape but may be crucial to the size of the coherence volume over which the excitation is delocalized. We conclude that a disordered linear chain Frenkel exciton model falls short to describe the line shape of the J band and the low-temperature superradiant dynamics at the same time.

Using the same one-dimensional exciton model, we have also calculated the density-of-states (DOS) function of the disordered band. Experimentally, this DOS function can be derived from temperature-dependent vibrational emission spectra. However, the line shape of the exciton-to-vibrational-band transition, shown in Fig. 9, does not allow any firm conclusion regarding the correctness of the one-dimensional exciton model. The broken curve in Fig. 9 presents the predicted spectrum based on the calculated DOS function with the same parameters as used for the line shape simulation. However, the emission spectrum is also consistent with a

Downloaded 06 Feb 2006 to 129.125.25.39. Redistribution subject to AIP license or copyright, see http://jcp.aip.org/jcp/copyright.jsp

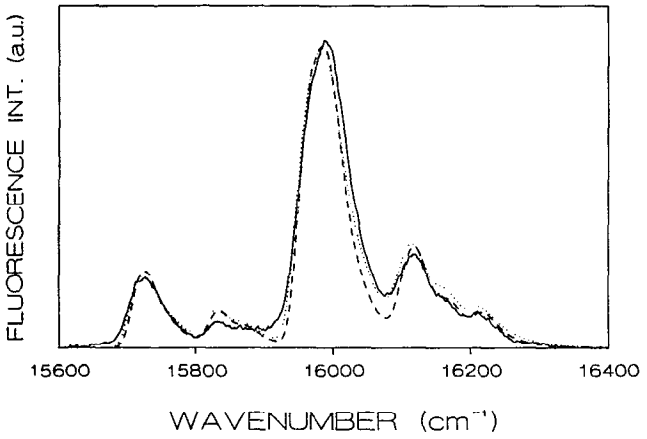

FIG. 9. Part of the fluorescence spectrum of the J aggregate (red site) (—) at 59 K, together with fits based on a two-dimensional (···) and one-dimensional (– –) density of states function for $J_{12} = -600\ \text{cm}^{-1}$ and $D = 64\ \text{cm}^{-1}$. Note that the smooth underground fluorescence has been subtracted.

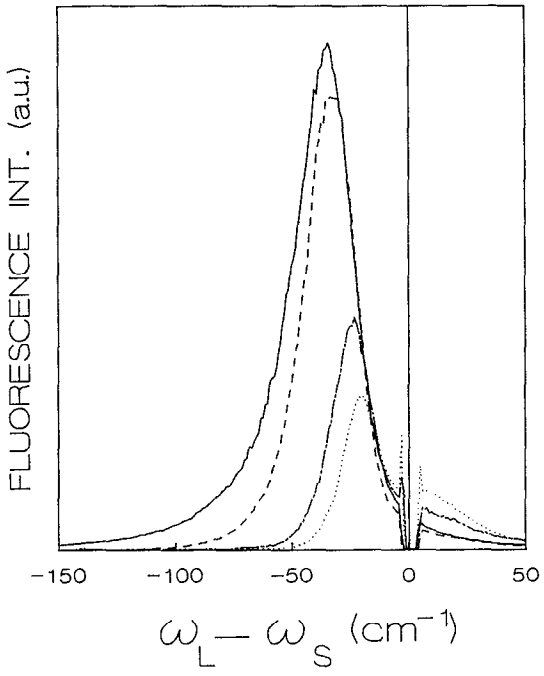

FIG. 11. Dephasing induced fluorescence profiles of the red site of PIC-Br at 77.5 K (—), 24.4 K (– –), 11.4 K (–·–), and 8.26 (···). The laser frequency is tuned 30 cm^{-1} below the absorption maximum, at all temperatures.

DOS function of a two-dimensional system as shown by the dotted curve in Fig. 9. It seems worthwhile to study the band structure of the aggregate by performing absorption experiments from a ground state vibrational level populated by stimulated emission pumping.

We now turn to a discussion of the resonance light scattering experiments on the red excitonic transition of PIC. RLS experiments on the blue excitonic origin of PIC are also possible but more difficult to analyze, because of overlap between the RLS spectrum with emission from the red site induced by absorption at the exciting laser wavelength. Figure 10 shows the fluorescence observed at 91 K when the exciting laser is tuned 30 cm^{-1} to the red of the energetically lowest J band. Note that the emission is observed on the *blue* side of the laser excitation wavelength. The insert in Fig. 10 shows RLS spectra at higher detection sensitivity at two different temperatures. At low temperature (1.5 K), one observes Raman bands only (the sharp peaks); at higher temperatures, one observes also fluorescence onto vibrational bands of the ground state potential energy surface. The nonobservation of dephasing induced emission at 1.5 K must be interpreted, according to Eq. (7), as clear evidence for the absence of *pure* dephasing processes at this temperature. This fact was used in the discussion of the difference between decay of the photon echo and the radiative decay of the system at low temperature (*vide retro*).

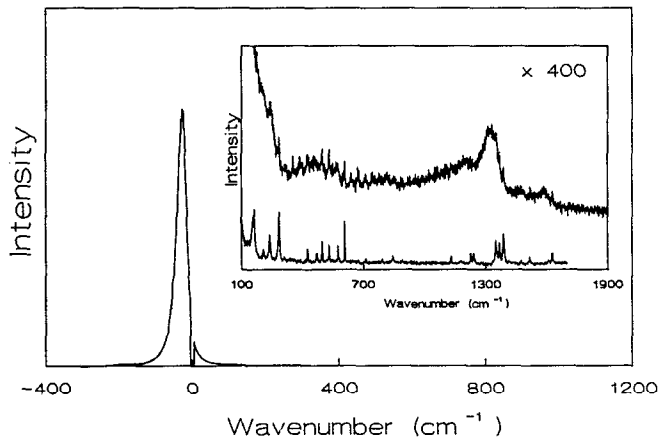

FIG. 10. RLS spectrum for the red site of PIC-Br at 1.5 and 91 K. The excitation frequency is 30 cm^{-1} below the absorption maximum. The dip at zero wave numbers arises from blocking the spectrometer at that frequency. The upper trace in the insert shows the vibronic fluorescence at the same excitation frequency, at 91 K. The lower trace is the RLS spectrum at 1.5 K.

Figure 11 shows how the line shape of the dephasing-induced origin emission changes as a function of temperature. The most interesting feature of Fig. 11 is that it shows that a state near the bottom of the band can be scattered by phonons to higher lying band states. The induced emission profiles are found to be consistent with a Boltzmann distribution among the band states. This observation holds even at 8 K, where the exciton–phonon scattering time constant is about 150 ps and much longer than the fluorescence lifetime of 70 ps. This implies that the cross section for scattering from the initially excited state to all states in the band is the same and that phonon scattering thus creates a Boltzmann distribution over the states in the band. Thus *all* thermally accessible band states participate in the optical dephasing process and no specific doorway state exists as was inferred from the temperature dependence of the photon echo decay time. We note that these observations imply also that optical dephasing occurs only through exciton–phonon scattering processes in the excited state, which leads to obeying of the condition given in Eq. (6). We finally note from Fig. 11 that

Downloaded 06 Feb 2006 to 129.125.25.39. Redistribution subject to AIP license or copyright, see http://jcp.aip.org/jcp/copyright.jsp

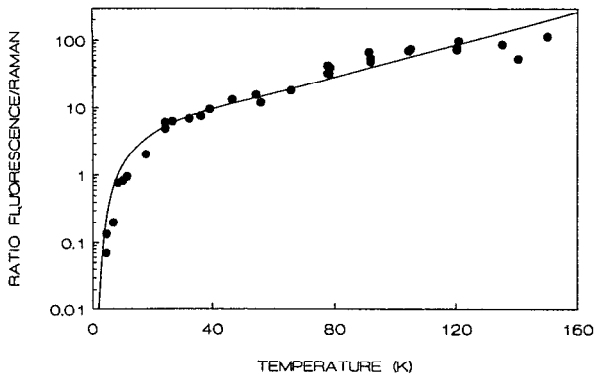

FIG. 12. Temperature dependence of the ratio of the vibronic fluorescence over Raman yields obtained for a frequency detuning of 30 cm^{-1} below the maximum of the red excitonic transition. The solid line gives the ratio $2T_1/T_2^*(T)$. It is based upon the best fit through the temperature dependent pure dephasing times, obtained from the accumulated photon echo data and the low-temperature fluorescence lifetime of 70 ps.

the J band, despite its inhomogeneous character, behaves as an exciton-band transition and not as a convolution of an excitonic transition and an inhomogeneity function.

Additional information about the exciton–phonon scattering process can be obtained from the ratio R between the Raman and fluorescence component in the RLS spectrum as discussed in Sec. II B. Figure 12 compares the measured temperature dependence of the vibrational fluorescence over Raman yields to the curve simulated on basis of the pure dephasing parameters extracted from the accumulated photon echo experiments and by using the fact that on resonance R equals $2T_1/T_2^*$ [Eq. (7)]. For the theoretical curve, which is based on Eq. (7), we have taken the low-temperature population (T_1) relaxation time because the Raman yield is not and the origin fluorescence yield is only slightly affected by the temporary storage of the population in the dark states of the band. The perfect fit of the data to the "theoretical" curve lends credence to our previous analysis of the temperature dependence of the photon echo decay. Note that in the low-temperature regime RLS is a more sensitive probe than the photon echo for *pure* dephasing processes because the photon echo measures both pure dephasing and population relaxation. To obtain the ratio between the vibrational fluorescence and Raman scattering yields the origin fluorescence yield and Raman yield of the 607cm^{-1} mode were determined. Using also the total integrated Raman yield and the Franck–Condon (FC) factor of the origin transition, the ratio of the fluorescence over Raman yields can be calculated. At 91 K, a FC factor of 0.98 was calculated from the emission spectrum. However, in order to obtain *quantitative* agreement between the pure dephasing data obtained from the RLS experiments and photon echo experiments a FC factor of 0.972 is needed. The difference between the two numbers is attributed to the low accuracy of the spectral determination of the FC factor.

Detailed information on the exciton dynamics can be obtained by a study of the frequency dependence of the RLS spectrum. Figure 13 shows three plots of the frequency dependence of the ratio of fluorescence over Raman yields for three different temperatures. The solid lines in these figures are fits based on Eq. (7) and taking into account the "inhomogeneity" of the line profile as discussed in Sec. II B. From the fits in Fig. 13, we have extracted the bath correlation function at different temperatures. The parameters defining this function are gathered in Table I. Noteworthy from this table is the fact that in all cases the condition $\Delta\tau_c \ll 1$ holds, which implies that the exciton's dynamics occurs in the *fast modulation* limit, making T_2^* a well-defined quantity. Table I also shows that Δ is approximately linear with temperature, which suggests that Δ is determined by the population of low-frequency phonons active in the scattering process. It is further tempting to interpret τ_c as the average lifetime of the "exciton–phonon" collision complex and Δ as a measure of the coupling strength of this compound state. To the best of our knowledge, this is the first time that RLS has been used to study molecular exciton de-

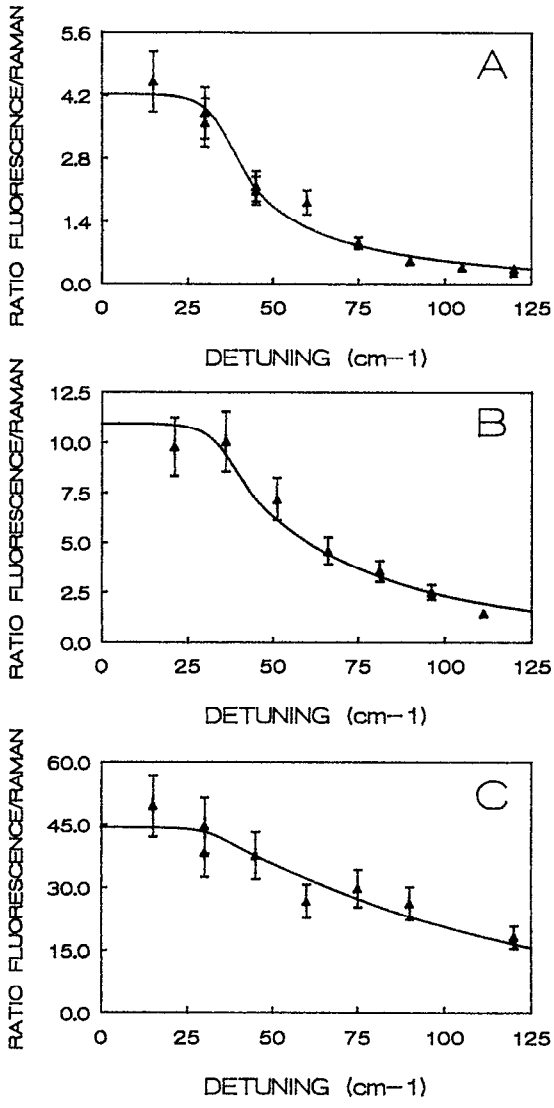

FIG. 13. Detuning dependence of the ratio of the vibronic fluorescence over Raman yields at 24.4 K (a), 39.4 K (b), and 77.5 K (c). Parameters of the fits are listed in Table I.

Downloaded 06 Feb 2006 to 129.125.25.39. Redistribution subject to AIP license or copyright, see http://jcp.aip.org/jcp/copyright.jsp

TABLE I. Parameters defining the bath correlation function.

T (K)	τ_c (fs)	Δ (cm^{-1})	$\Delta\tau_c$	Δ/k_BT
24.4	151^{+40}_{-25}	2.7 ± 0.5	0.08 ± 0.02	0.16 ± 0.03
39.4	106 ± 15	4.4 ± 0.9	0.09 ± 0.02	0.16 ± 0.03
77.5	59 ± 10	9.8 ± 2.0	0.11 ± 0.03	0.18 ± 0.04

phasing and that the mechanism by which the exciton loses its phase memory has been unravelled.

We will now discuss the optical dynamics of PIC-I in a LB film. The absorption and emission spectra of a bilayer of PIC-I at 77 K are shown in Fig. 14. The first thing to note is that the position of the J band is only slightly shifted compared to the glass but that the spectral width of the J band in an LB film is much larger than in an ethylene glycol/water glass. We suggest that the main cause for the difference in widths of the J bands is due to a larger disorder present in the LB films. Support for this analysis comes from a line shape simulation of the J band in the film. Using the same linear chain model with a nearest-neighbor coupling of -600 cm^{-1} and a diagonal disorder D of 260 cm^{-1} the lineshape of the J band can be reproduced. While these numbers in themselves are not unique they suffice to show that in these LB films the disorder is substantially larger than for aggregates in the ethylene glycol/water glass. We further note that unlike the glass spectrum the absorption spectrum of PIC in the LB film looks smooth and exhibits little vibronic structure and no sign of an upper bandedge. In fact, the very weak shoulder at 530 nm may not belong to the aggregate's absorption spectrum because its intensity depends on the sample quality and it does not show up in a fluorescence excitation spectrum when the emission is detected at 600 nm. However, when the emission is detected more to the blue, for instance at 590 nm, the peak at 530 nm is observed. These findings show that the band structure of PIC in a LB film is different from the one in self-organized aggregates in a glass. It suggests also that vibronic coupling is reduced in a LB film which may be the result of more extensive delocalization of the excitation in this quasi two-dimensional structure. Figure 14 also shows that the emission spectrum of PIC in the bilayer at 77 K is narrowed compared to the absorption spectrum. We attribute this effect to fast exciton relaxation at energies above the renormalized band edge. Fluorescence decay curves of a bilayer of PIC at 1.5 K detected at different wavelengths are shown in Fig. 15. These deconvoluted fluorescence decay curves show that the decay is nonexponential with an initial fast component of about 10 ps when the emission is detected at the maximum of the emission spectrum. On the blue side of the band the initial decay is faster, on the red side slower. The decay curves in Fig. 15 permit also the conclusion that the "average" decay time becomes longer when the detection wavelength becomes greater. However, the time resolution in these experiments does not allow a precise determination of the fast relaxation constants. We note that these results are in line with earlier measurements by Dorn and Müller[52] of the fast component in the decay of PIC in an LB film, who used a high-power laser for excitation and a streak camera for detection of the emission. The nonexponentiality of the decay curves is attributed to a combination of transport and radiative decay. A more quantitative analysis of these effects is underway. As mentioned earlier, Gruhl *et al.*[50] showed that the fluorescence quantum yield of these PIC aggregates in an LB film is near unity, except for the red edge of the J band where it is 0.8. In an exciton band picture of the J line this effect can be understood by recalling that in the calculations the most radiant states are found near the bottom of the band. Consequently, the Förster energy-transfer rate to traps below the band will be largest for excitonic states near the bottom of the band. From the aforementioned lifetime measurements, we conclude that in the PIC bilayer the optical excitation is much more delocalized than in the self-organized aggregates. The dimensionality of the system thus plays a crucial role in the dynamics.

We have also used RLS spectroscopy to probe the dynamics of PIC aggregates in a bilayer. A comparison

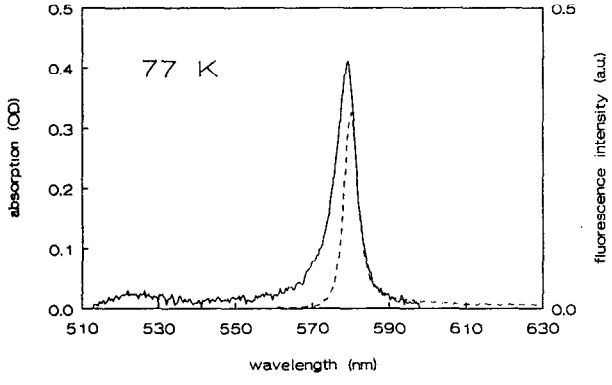

FIG. 14. Absorption (—) and emission (– –) spectrum of a bilayer LB film of PIC-I, both measured at 77 K. The fluorescence excitation wavelength was 560 nm.

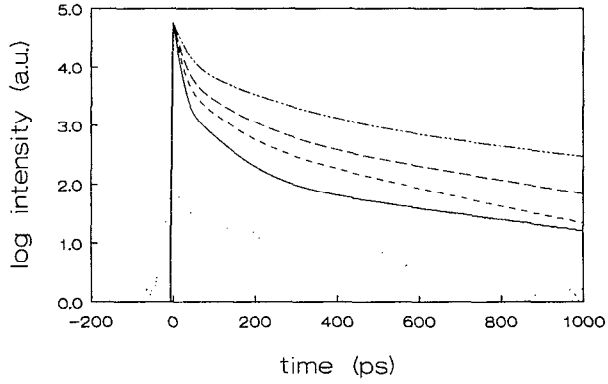

FIG. 15. Wavelength dependence of the fluorescence decay of a bilayer LB film of PIC-I at 1.5 K. The decay times (initial height) of the fast component of the deconvoluted decay curves are 9 ps (0.96) at 574 nm (—); 11 ps (0.91) at 581 nm (– –); 14 ps (0.89) at 584 nm (— —) and 21 ps (0.81) at 589 (— – — –). The dotted curve represents the instrument response.

Downloaded 06 Feb 2006 to 129.125.25.39. Redistribution subject to AIP license or copyright, see http://jcp.aip.org/jcp/copyright.jsp

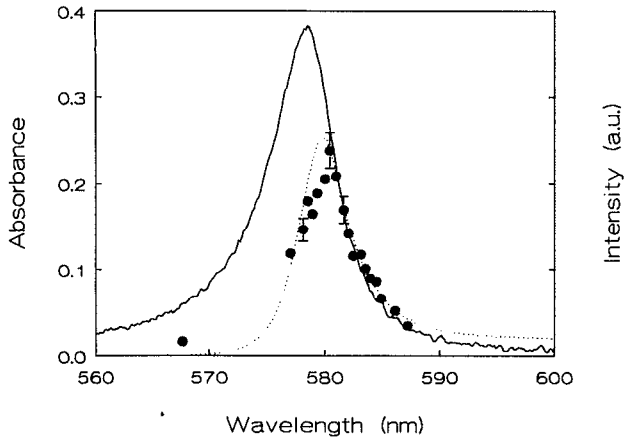

FIG. 16. Comparison between the absorption spectrum (- -), resonance Rayleigh scattering spectrum (●), and fluorescence spectrum (···) of a bilayer of PIC-I at 77 K.

between the absorption and resonance Rayleigh scattering spectrum of the PIC bilayer at 77 K is shown in Fig. 16. Scattered laser light as the source for the resonance scattered light can be excluded because of the fact that by tuning the laser out of resonance the intensity of the scattered light drops to a few percent of the resonance value. Figure 16 clearly shows that the relative intensity of the Rayleigh scattering decreases dramatically above the renormalized band edge. Recent Rayleigh scattering experiments have also shown that the blue tail of the Rayleigh spectrum decays smoothly to the baseline. Using Eq. (8), we attribute the collapse of the Rayleigh spectrum on the high-energy side of the absorption spectrum to shortening of the dephasing time T_2 for states above the band edge, which probably results from a greater mobility of excitons in this part of the band. It is interesting to notice in Fig. 16 that the fluorescence spectrum of the PIC bilayer basically tracks the resonance Rayleigh scattering spectrum, confirming the fact that a change in exciton dynamics above the band edge is the key point to understanding of both the Rayleigh and fluorescence spectra. The spectra shown in Fig. 16 strongly suggest that the renormalized band edge marks a "mobility edge" in this aggregate system. We have also found that when the PIC bilayer is cooled down to 1.5 K, the absorption, fluorescence, and resonance Rayleigh scattering spectra show a substantial broadening, which reverses upon warming up to 298 K. This effect is, most likely, due to an increased disorder of the system, caused by a different contraction of the film and the substrate. The PIC bilayer seems therefore extremely suitable for a detailed understanding of the relation between exciton dynamics and disorder. Finally, accumulated photon echo experiments on the PIC bilayer have confirmed that the exciton dephasing rate above the band edge is much faster than below the edge. Experiments are underway to investigate the dynamics of the PIC bilayer and monolayer in greater detail.

These preliminary results, however, amply demonstrate that resonance Rayleigh scattering is a powerful tool for the study of the frequency-dependence of exciton dephasing in aggregates and polymers.

V. SUMMARY AND CONCLUSIONS

Using a variety of nonlinear optical measurement techniques and numerical calculations, we have shown that the J band in aggregates of PIC in glasses and LB films can be described in terms of a disordered Frenkel exciton band. Excitonic states, delocalized over about 100 molecules and carrying giant oscillator strengths, have been shown to exist below the renormalized band edge. These states are superradiant at low temperature. The superradiant behavior of these excitonic states is shown to be limited by disorder at low temperature and by exciton–phonon scattering at higher temperatures, but the precise mechanism for the temperature dependence of the superradiant effect is still in question. We have further shown that the exciton dynamics of PIC in a glass occurs in the *fast modulation limit* and that the exciton dynamics in a film of PIC changes rather abruptly at the renormalized band edge. It has also been demonstrated that resonance light scattering is a powerful tool for the study of exciton dynamics in aggregates and polymers.

ACKNOWLEDGMENTS

We are indebted to F. de Haan for providing the programs for instrument control and data analysis. We also thank Dr. A. J. Schouten of the Polymer Chemistry Group for use of the Langmuir–Blodgett film growth facility. We gratefully acknowledge stimulating discussions with Dr. K. E. Drabe on resonance Rayleigh scattering. The investigations were supported by the Netherlands Foundation for Chemical Research (SON) and Physical Research (FOM) with financial aid from the Netherlands Organization for the Advancement of Science (NWO).

[1]E. Hanamura, Phys. Rev. B **37**, 1273 (1988).
[2]Y. Wang, Chem. Phys. Lett. **126**, 209 (1986).
[3]S. E. Rickert, J. B. Lando, and S. Ching, in *Nonlinear Optical Properties of Organic and Polymeric Materials*, Chap. 11 (ACS Symposium series 233, American Chemical Society, 1983).
[4]H. Kuhn, D. Möbius, and H. Bücher, in *Techniques in Chemistry*, Vol. 1, Part III B, p. 577ff (Wiley-Interscience, New York, 1972).
[5]S. de Boer, K. J. Vink, and D. A. Wiersma, Chem. Phys. Lett. **137**, 99 (1987).
[6]S. de Boer and D. A. Wiersma, Chem. Phys. **131**, 135 (1989).
[7]S. de Boer and D. A. Wiersma, Chem. Phys. Lett. **165**, 45 (1990).
[8]H. Fidder, J. Knoester, and D. A. Wiersma, Chem. Phys. Lett. **171**, 529 (1990).
[9]R. D. Miller and J. Michl, Chem. Rev. **89**, 1359 (1989).
[10]Y. R. Kim, M. Lee, J. R. Thorne, R. M. Hochstrasser, and J. M. Zeigler, Chem. Phys. Lett. **145**, 75 (1988).
[11]J. R. G. Thorne, Y. Osaka, J. M. Zeigler, and R. M. Hochstrasser, Chem. Phys. Lett. **162**, 455 (1989).
[12]H. P. Trommsdorff, J. M. Zeigler, and R. M. Hochstrasser, J. Chem. Phys. **89**, 4440 (1988).
[13]A. Tilgner, H. P. Trommsdorff, J. M. Zeigler, and R. M. Hochstrasser, J. Lumin. **45**, 373 (1990).
[14]E. E. Jelley, Nature (Lond.) **138**, 1009 (1936); Nature (Lond.) **139**, 631 (1937).
[15]G. Scheibe, Angew. Chem. **49**, 563 (1936); Angew. Chem. **50**, 212 (1937).
[16]G. Scheibe, in *Optische Anregungen organischer Systeme*, edited by W. Först (Verlag Chemie, Weinheim, 1966), p. 109ff.

Downloaded 06 Feb 2006 to 129.125.25.39. Redistribution subject to AIP license or copyright, see http://jcp.aip.org/jcp/copyright.jsp

[17]E. Daltrozzo, G. Scheibe, K. Gschwind, and F. Haimerl, Phot. Sci. Eng. **18**, 441 (1974).
[18]D. L. Smith, Phot. Sci. Eng. **18**, 309 (1974).
[19]E. W. Knapp, Chem. Phys. **85**, 73 (1984).
[20]P. O. J. Scherer and S. F. Fischer, Chem. Phys. **86**, 269 (1984).
[21]E. W. Knapp, P. O. J. Scherer, and S. F. Fischer, Chem. Phys. Lett. **111**, 481 (1984).
[22]D. L. Huber, Chem. Phys. **128**, 1 (1988).
[23]F. C. Spano and S. Mukamel, J. Chem. Phys. **91**, 683 (1989).
[24]J. Grad, G. Hernandez, and S. Mukamel, Phys. Rev. A **37**, 3835 (1988).
[25]F. C. Spano, J. R. Kuklinski, and S. Mukamel, Phys. Rev. Lett. **65**, 211 (1990).
[26]V. Sundström, T. Gillbro, R. A. Gadonas, and A. Piskarskas, J. Chem. Phys. **89**, 2754 (1988).
[27]R. Hirschmann and J. Friedrich, J. Chem. Phys. **91**, 7988 (1989).
[28]R. Hirschmann, W. Köhler, J. Friedrich, and E. Daltrozzo, Chem. Phys. Lett. **151**, 60 (1988).
[29]D. Möbius and H. Kuhn, Isr. J. Chem. **18**, 375 (1979).
[30]S. K. Rentsch, R. V. Danielius, R. A. Gadonas, and A. Piskarskas, Chem. Phys. Lett. **84**, 446 (1981).
[31]Z. X. Yu, P. Y. Lu, and R. R. Alfano, Chem. Phys. **79**, 289 (1983).
[32]P. W. Anderson, Phys. Rev. **109**, 1492 (1958).
[33]A. S. Davydov, *Theory of Molecular Excitons* (Plenum, New York, 1971).
[34]J. Klafter and J. Jortner, J. Chem. Phys. **68**, 1513 (1978).
[35]D. M. Burland, U. Konzelmann, and R. M. Macfarlane, J. Chem. Phys. **67**, 1926 (1977).
[36]M. Schreiber and Y. Toyozawa, J. Phys. Soc. Jpn. **51**, 1528 (1982); *ibid.* **51**, 1537 (1982).
[37]E. I. Rashba and G. E. Gurgenishvilli: Sov. Phys.-Solid State **4**, 759 (1962).
[38]H. Fidder and D. A. Wiersma (to be published).
[39]D. L. Huber, Phys. Rev. **158**, 843 (1967); **170**, 418 (1968); **178**, 93 (1969); **187**, 392 (1969); **B1**, 3409 (1970).
[40]R. M. Hochstrasser and F. A. Novak, Chem. Phys. Lett. **48**, 1 (1977); Chem. Phys. Lett. **53**, 3 (1978); R. M. Hochstrasser, F. Novak, and C. A. Nyi, Isr. J. Chem. **16**, 250 (1977).
[41]J. Hegarty, M. D. Sturge, C. Weisbuch, A. C. Gossard, and W. Wiegmann, Phys. Rev. Lett. **49**, 930 (1982).
[42]P. de Bree, thesis, University of Groningen (1981).
[43]A. Ron and A. Ron, Chem. Phys. Lett. **58**, 329 (1978).
[44]S. Mukamel, J. Chem. Phys. **71**, 2884 (1979).
[45]R. Kubo, in *Fluctuation, Relaxation and Resonance in Magnetic Systems*, edited by D. Ter Haar (Oliver and Boyd, Edinburgh, 1962), p. 23; Adv. Chem. Phys. **15**, 101 (1969).
[46]F. J. Schmitt and W. Knoll, Chem. Phys. Lett. **165**, 54 (1990).
[47]W. H. Press, B. P. Flannery, S. A. Teukolsky, and W. T. Vettering, *Numerical Recipes* (Cambridge University, New York, 1987), Chaps. 7 and 11.
[48]D. L. Akins and J. W. Macklin, J. Phys. Chem. **93**, 5999 (1989).
[49]Y. Toyozawa, Prog. Teoret. Phys. **20**, 53 (1958).
[50]H. Gruhl, H.-P. Dorn, and K. Winzer, Appl. Phys. B **38**, 199 (1985).
[51]J. Feldmann, G. Peter, E. O. Göbel, P. Dawson, K. Moore, C. Foxon, and R. J. Elliott, Phys. Rev. Lett. **59**, 2337 (1987).
[52]H.-P. Dorn and A. Müller, Appl. Phys. B **43**, 167 (1987).

Downloaded 06 Feb 2006 to 129.125.25.39. Redistribution subject to AIP license or copyright, see http://jcp.aip.org/jcp/copyright.jsp